Novel in situ NMR Measurement System for Evaluating Molecular Mobility during Drawing from Highly Entangled Polyethylene Melts[a]

Masaki Kakiage, Hiroki Uehara,* Takeshi Yamanobe

A novel in situ measurement system for evaluating molecular mobility during uniaxial drawing of polymeric materials was established by introducing drawing and stress-detecting devices into a ^{1}H pulse nuclear magnetic resonance spectrometer. In this study, we analyze the changes in molecular motion of amorphous chains during melt-drawing of ultra-high molecular weight polyethylenes (UHMW-PEs) with different molecular weight distributions. In the initial stage of drawing, a three-component resolution was possible for the relaxation decay curve, which includes "rigid", "intermediate", and "mobile" amorphous components. The quality and quantity changes in these components demonstrated that this intermediate amorphous component could be regarded as the index of the change in molecular entanglement characteristics during the orientation of PE chains.

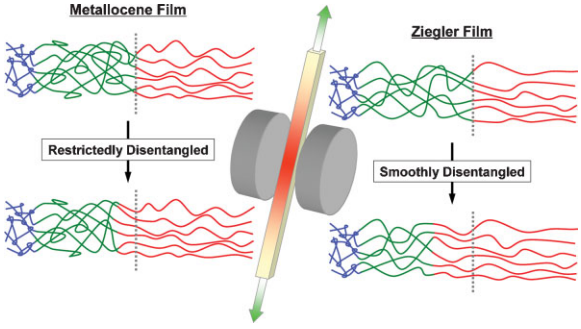

Introduction

Ultra-high molecular weight polyethylene (UHMW-PE) can be drawn even from the molten state using its higher melt viscosity.[1–5] Transient crystallization into a hexagonal form occurs during oriented crystallization into a final orthorhombic form during melt-drawing of UHMW-PE, as determined by in situ wide-angle X-ray diffraction (WAXD) measurements using synchrotron radiation.[6] Furthermore, we examined the correlation between this transient crystallization and molecular entanglement characteristics of the sample films, i.e., MW or MW distribution (MWD).[7,8] In particular, the difference in MWD dominated the phase development mechanism during melt-drawing.[7,9] The obtained results suggested that structural transformation of amorphous chains induces transient crystallization into the hexagonal form. Namely, oriented crystallization occurred through disentanglement of chains in the melt-drawing process.

Consequently, in situ measurement of the change in the amorphous structure during melt-drawing is important for understanding the characteristic phase development mechanism. However, WAXD measurement is not appropriate for analyzing amorphous structures, although it is a good tool for analyzing crystalline structures. Thus, it is

M. Kakiage, H. Uehara, T. Yamanobe
Department of Chemistry and Chemical Biology,
Gunma University, Kiryu, Gunma 376-8515, Japan
E-mail: uehara@chem-bio.gunma-u.ac.jp
M. Kakiage
Research Fellow of the Japan Society for the Promotion of Science,
Present address: Tokyo Institute of Technology, Ookayama,
Meguro-Ku, Tokyo 152-8552, Japan

[a] Supporting information for this article is available at the bottom of the articles abstract page, which can be accessed from the journal's homepage at http://www.mrc-journal.de, or from the author.

DOI: 10.1002/marc.200800316

necessary to develop a novel in situ measurement system to detect changes in amorphous structures.

Direct measurement of the amorphous phase is limited to a few spectroscopic methods, i.e., nuclear magnetic resonance (NMR),[10–32] infrared,[33–35] and Raman spectroscopy.[36,37] Sensibility on a microscale is required in order to discuss the correlation with structural transformation. Furthermore, it has been revealed that a transient mesophase, that is a boundary between amorphous and crystal, also arises with melt-drawing. Considering these analytical requirements, NMR spectroscopy is the most suitable method for the in situ measurement system in this study. One of the features of NMR analysis is possible component resolution of non-crystalline phase based on the difference in relaxation time. We previously reported that ^{1}H pulse NMR measurement was useful for evaluating the amorphous structure and mesophase of UHMW-PE samples,[23,24,26,32] which is difficult to do using X-ray measurements.

NMR spectroscopy can be applied in in situ measurements during deformation.[21,22,25,27,30] Gleason et al.[22] investigated the effect of uniaxial deformation near the glass transition temperature on the chain mobility in the amorphous region of deuterated nylon 6. Rault et al.[30] studied the stress-induced crystallization and melting of cross-linked rubber. However, oriented crystallization from the molten state of semi-crystalline polymer, which probably contains disentanglement of chains, is not revealed. Therefore, in this study, we attempt to analyze the molecular motion of amorphous chains during melt-drawing of UHMW-PE, based on in situ NMR measurement. Two types of UHMW-PEs polymerized by metallocene and Ziegler catalyst systems, which give different MWDs even if they have comparable MW, were selected in this study. Quantitative evaluation of the effect of MWD on chain disentanglement behavior was also examined.

Experimental Part

Materials

Two types of UHMW-PE materials were supplied by Asahi Kasei Chemicals Co. They were prepared using a metallocene catalyst system with viscosity average MWs ($\overline{M}_v$) of $1.07 \cdot 10^7$ g $\cdot$ mol^{-1} and a Ziegler catalyst system with $\overline{M}_v$ of $1.00 \cdot 10^7$ g $\cdot$ mol^{-1}. These materials featured a narrower MWD for the metallocene-catalyzed material and a broader MWD for the Ziegler-catalyzed material. Gel permeation chromatography (GPC) measurements were performed on these materials, but components with MWs exceeding 10^7 g $\cdot$ mol^{-1} cannot be detected by the GPC method. Thus, an accurate analysis of the MWDs of these materials was difficult.

Sample Preparation

These UHMW-PE materials were compression-molded into films at 180 °C and 30 MPa for 10 min, followed by slow cooling to room temperature. Antioxidants, namely 0.5 wt.-% (based on polymer) of both octadecyl 3-(3,5-di-*tert*-butyl-4-hydroxyphenyl)propanoate and bis(2,4-di-*tert*-butylphenyl)pentaerythritol diphosphite, were added to each material with an appropriate amount of acetone. The resultant film thickness was 3.5 mm. A 3.5 mm square prismatic specimen was cut from these compression-molded films.

Melt-Drawing

All melt-drawings were made at 150 °C, well above the sample melting temperature (135 °C). Before drawing, the sample specimen was held at 150 °C for 10 min for temperature equilibrating. The cross-head speed of drawing was always 2 mm $\cdot$ min^{-1}.

Measurements

In situ ^{1}H pulse NMR measurements during melt-drawing were performed using a JEOL MU-25 solid-state pulse NMR spectrometer operating at 25.0 MHz. The relaxation decay was recorded using the Carr-Purcell-Meiboom-Gill (CPMG) pulse sequence,[38] which is suitable for samples with long spin-spin relaxation time (T_2) such as molten amorphous or elastomers.[20] Thus, we selected this detecting method to analyze the amorphous change during melt-drawing in this study. The 90° pulse length was 4.0 μs and the repetition time was 5.0 sec.

Results and Discussion

First, an in situ NMR measurement system for evaluating molecular mobility during melt-drawing was developed (see Figure S1 in Supporting Information). Samples were drawn using our designed uniaxial cross-head extension device, which can be installed in an NMR spectrometer. Two cross-heads of this extension device move in opposite directions perpendicular to the magnetic field. Thus, the center region of the sample specimen is always in a detection coil, which is located at the center of the magnet. The stress during the melt-drawing process was recorded using a load cell (Kyowa Electronic Instruments Co., Ltd., LUR-A-100NSA1) installed in the extension device.

The sample was heated by a heat blower attached to the NMR probe system (see Figure S2 in Supporting Information). Heated air was blown parallel to the magnetic field on the detection coil in the probe through a poly(tetrafluoroethylene) channel. Thus, the most drawn region is the same as the detecting position of the NMR signal and drawing stress because the heated air blows only around the detection coil. The measurement temperature was calibrated by a thermocouple placed at the center of the probe before drawing.

It was previously reported that melt-drawing of UHMW-PE produces a unique stress-strain behavior, that is a

Macromolecular Journals
DOI: 10.1002/marc.200800316

plateau stress phenomenon in the early stage of the draw, followed by a strain-hardening region with oriented crystallization.[2,3,5–8] This plateau stress region was also observed for both films examined in this study (see Figure S3 in Supporting Information). Thus, deformation from the complete amorphous state was achieved during melt-drawing of UHMW-PE at 150 °C using this in situ NMR measurement system. As mentioned before, the CPMG pulse sequence is suitable for evaluating the longer T_2 component, i.e., amorphous phase, but cannot detect the shorter T_2 component, i.e., crystalline phase. Therefore, this in situ NMR analysis was applied before the plateau stress (≈2 000 sec) because only an orientation of amorphous chains occurred in this strain region, as revealed by our previous in situ WAXD measurements.[6–8]

Figure 1 indicates the changes in observed NMR relaxation decay curves recorded using the CPMG pulse sequence with drawing time for both films. A large difference in the slope is observed around a relaxation time of 10 ms, and its intensity gradually increases with drawing time. Here, T_2 was estimated from these relaxation decay curves by curve fitting. A Lorentz-type fitting function (Equation 1), which is usually used to analyze the amorphous component in a semi-crystalline polymer, was selected for the fitting function in this study.

$$I(t) = A \exp\left(-\frac{t}{T_2}\right) \quad (1)$$

Generally, several components contribute to the relaxation decay for a polymer material because heterogeneous structures essentially exist even in the amorphous state. Thus, the obtained relaxation decay was resolved into several components. Functional resolution assuming two or three components was performed for the relaxation decay curves obtained in this study.

Figure 2 depicts the instance of curve fitting for a relaxation decay curve recorded at a drawing time of 80 s

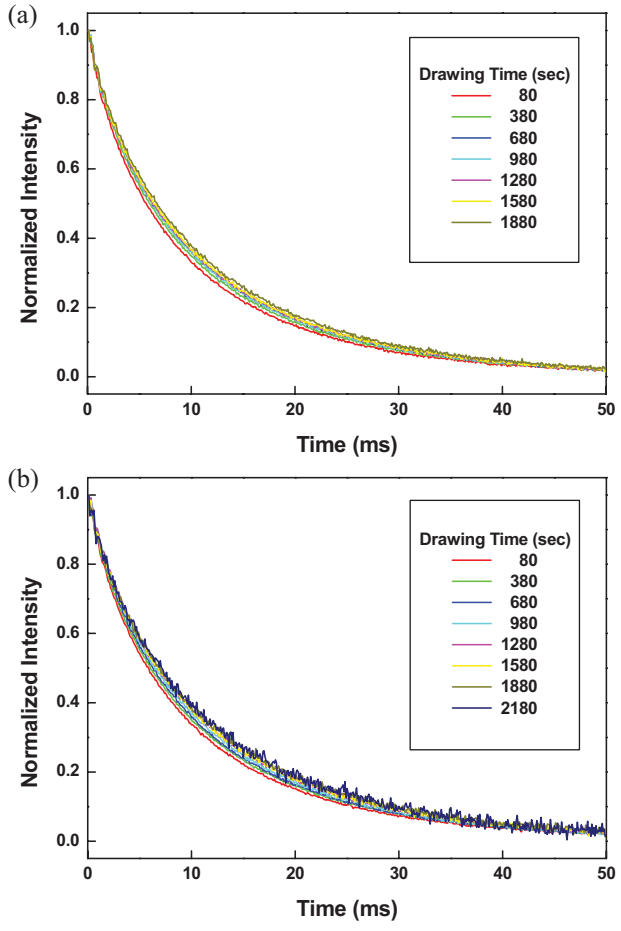

Figure 1. Changes in relaxation decay curves recorded using CPMG pulse sequence during melt-drawing at 150 °C for (a) metallocene and (b) Ziegler films.

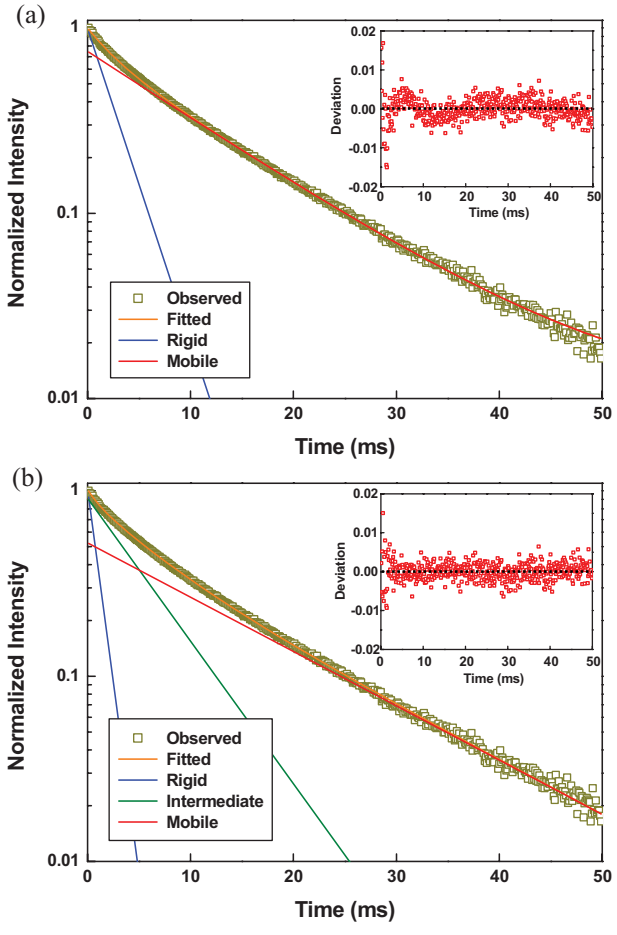

Figure 2. Comparison of curve-fitting results for relaxation decay curve recorded at drawing time of 80 sec for metallocene film, assuming (a) two- and (b) three-component resolutions. Inset figures depict the deviation of the fitting value from the experiment value.

for the metallocene film. Comparing experiment and fitting curves, the resolution assuming three components (Figure 2b) is suitable for this relaxation decay curve, although that assuming two components (Figure 2a) has a statistical error. This three-component resolution was suitable for all the other decay curves. Therefore, curve fitting assuming three components was adopted for the series of relaxation decay curves obtained in this study. Three amorphous components were defined as rigid (shortest T_2), intermediate, and mobile (longest T_2). Figure 3 illustrate the changes in the component ratio of each component for the metallocene and Ziegler films during melt-drawing. For the change in T_2 depicted (see Figure S4 in Supporting Information), the Ziegler film exhibits higher values for all components than the metallocene film. This indicates that the chain mobility for the Ziegler film is higher than that for the metallocene film. However, these values hardly change during melt-drawing for both films.

An obvious difference in component ratio between the metallocene and Ziegler films is observed for the intermediate and mobile amorphous components (Figure 3). Comparing the initial drawing stage, the mobile amorphous component is predominant for the metallocene film. In contrast, the intermediate amorphous component is predominant for the Ziegler film. With drawing, an increase in the mobile amorphous component and a decrease in the intermediate amorphous component are observed for both films. These opposite phenomena mean that structural transformation from intermediate into mobile amorphous components occurs during melt-drawing. In particular, this structural transformation is more significant for the Ziegler film. However, the rigid amorphous component hardly changes even for the component ratio during melt-drawing for both films. As previous reported, no oriented crystallization occurs in this strain region before the plateau stress occurs.[6–8]

It is suggested that extensive disentanglement with chain slippage proceeds at the initial stage of melt-drawing for a Ziegler film with broader MWD.[6,7] The mobile amorphous component is attributed to the disentangled chains transformed from the prior intermediate amorphous component considering that this component significantly increases at the same stage for the Ziegler film. In contrast, the intermediate amorphous component with less mobility than the mobile amorphous component can be construed as networked amorphous chains connected by entanglements and distributed homogeneously over the whole chain. The rigid amorphous component has much lower chain mobility, that is shorter T_2. Thus, this component consists of entanglements tightly confining each other.

Models for structural transformation of amorphous chains are proposed in Figure 4 based on the experimental results of these in situ NMR measurements. The rigid amorphous component with $T_2 \approx 1$ ms (blue chains) can be defined as amorphous chains with tight entanglements that transfer the drawing stress well. The intermediate amorphous component with $T_2 \approx 5$ ms (green chains) can be defined as amorphous chains with loose entanglements, and the mobile amorphous component with $T_2 \approx 15$ ms (red chains) can be defined as disentangled amorphous chains. Significant structural transformation from intermediate into mobile amorphous components occurs during melt-drawing for the Ziegler film. Here, a Ziegler material with broader MWD includes a larger amount of lower MW component compared with a metallocene material with narrower MWD. Consequently, the intermediate amorphous component for the Ziegler film has looser entanglements (Figure 4b, green chains)

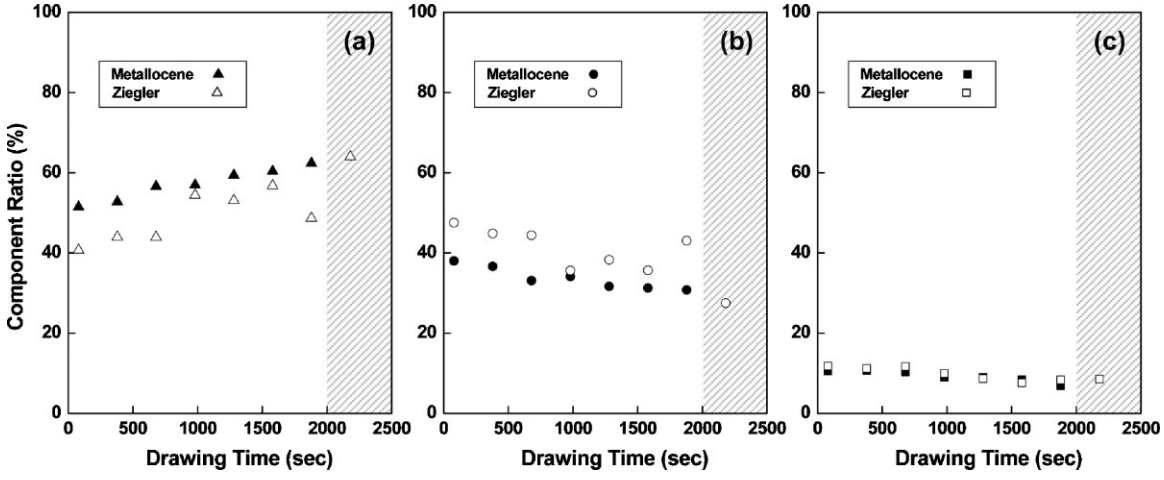

Figure 3. Changes in component ratio evaluated from the relaxation decay curves in Figure 1 for metallocene (filled symbols) and Ziegler films (open symbols): (a) Mobile, (b) intermediate, and (c) rigid amorphous components. The shaded area indicates the plateau stress region.

Macromol. Rapid Commun. **2008**, *29*, 1571–1576

DOI: 10.1002/marc.200800316

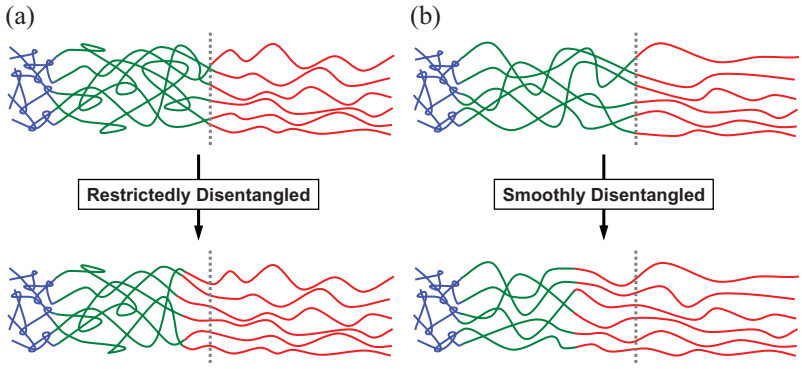

Figure 4. Models for structural transformation of amorphous chains for (a) metallocene and (b) Ziegler films. Blue, green, and red chains indicate rigid, intermediate, and mobile amorphous components. Top and bottom models represent the state before and after drawing. Gray dotted lines indicate the boundary between intermediate and mobile amorphous components at the state before drawing. Chain shape and length for each component in each model reflect T_2 and the component ratio estimated from in situ NMR measurement. There is a small disentangled region for metallocene film (a) with lower chain mobility because disentanglement of the intermediate amorphous component is "restricted". In contrast, the corresponding region is larger for Ziegler film (b) with higher chain mobility due to "smooth" disentanglement of the intermediate amorphous component.

than that for the metallocene film (Figure 4a, green chains). Indeed, the Ziegler film exhibited slightly higher T_2's than the metallocene film for both intermediate and mobile amorphous components (see Figure S4 in Supporting Information). Namely, broader MWD of the Ziegler film enhances the chain mobility in both T_2 levels. Thus, chains disentangle more smoothly during melt-drawing for the Ziegler film (Figure 4b). This means that the continuity of MWD for the Ziegler film induces the cooperation of the intermediate and mobile amorphous components during chain disentanglement. In contrast, a metallocene material with narrower MWD includes only a higher MW component. Thus, disentanglement of the intermediate amorphous component is restricted due to lower chain mobility with entanglements, and structural transformation is less pronounced for the metallocene film (Figure 4a). No structural transformation of the rigid amorphous component occurs during melt-drawing for either film due to the confinement of chains with tight entanglements. Here, in the result of NMR measurement for normal MW PE melt, no rigid amorphous component was recognized. Instead, a new amorphous component with much longer T_2 (≈94 ms) was observed for this sample, which is attributed to the lower MW segments with no entanglement or chain ends (see supplemental data in Supporting Information). In contrast, the rigid amorphous component is characteristic for UHMW-PE material, which always exists independent of induced deformation. Thus, this component is defined as the state with highly entangled chains. These results demonstrate that the difference in degree of chain disentanglement can be evaluated by in situ NMR measurement. Such a direct observation of the amorphous components is impossible for X-ray measurement. In particular, chain mobility of the intermediate amorphous component, i.e., loose entanglements, is equivalent to the ease of disentanglement. Therefore, the quality and quantity, i.e., T_2 and component ratio, of the intermediate amorphous component can be regarded as the indices of molecular entanglement characteristics of polymeric chains.

The T_2 and component ratio of the rigid amorphous component hardly changed during melt-drawing for both films. This rigid amorphous component with tight entanglements mainly transfers the tensile stress in a melt-drawing process. Therefore, chain entanglement estimated from an established mechanical analysis corresponds to this rigid amorphous component that dominates the stress transfer in the molten state. In contrast, the intermediate and mobile amorphous components with looser entanglements cannot be detected by such a mechanical analysis, due to their less effective contribution to the stress transfer than the rigid amorphous component. However, structural transformation from intermediate into mobile amorphous components occurred during melt-drawing, as analyzed by in situ NMR measurement in this study. These phenomena mean that these intermediate and mobile amorphous components can be elicited only by major deformation with chain disentanglement such as melt-drawing. Chain entanglement characteristics, including the change in entangled state, can be evaluated by this in situ NMR measurement during melt-drawing, which is different from characteristics essentially evaluated by mechanical measurement. This is the first study to directly observe the existence of entanglements with different roles for structural development, although it was suggested from the oriented crystallization behavior in a strain-hardening region during melt-drawing, i.e., an application for much larger deformations.[2]

Chain entanglement is typically analyzed by a rheological method using the plateau modulus. A critical MW giving entanglements is estimated by this analysis, assuming that chain entanglement remains unchanged. In contrast, chain disentanglement, i.e., the change in entangled state, occurs during major deformations such as melt-drawing. The change in chain entanglement characteristics during melt-drawing can be evaluated by the difference in relaxation time in this study for developing a novel in situ NMR measurement system consisting of a

melt-drawing device installed in an NMR spectrometer that can detect the structural transformation of amorphous chains.

Conclusion

A novel in situ NMR measurement system for evaluating molecular mobility during melt-drawing was established by introducing drawing and stress-detecting devices into an NMR spectrometer. Chain disentanglement during melt-drawing of UHMW-PE was evaluated using the CPMG pulse sequence. The relaxation decay curve could be resolved into three components, rigid, intermediate, and mobile amorphous components. Significant structural transformation from intermediate into mobile amorphous components occurred during melt-drawing for the sample with broader MWD because the chain mobility of the intermediate amorphous component was higher. These results demonstrate that the intermediate amorphous component is an index representing the change in molecular entanglement characteristics during melt-drawing of UHMW-PE.

Acknowledgements: This work was partly supported by a Grant-in-Aid for *the Japan Society for the Promotion of Science (JSPS) Fellows* and *the Industrial Technology Research Grant Program* in '04 from *the New Energy and Industrial Technology Development Organization (NEDO) of Japan*. M. Kakiage expresses his gratitude for the JSPS Research Fellowships for Young Scientists.

Received: May 21, 2008; Revised: July 21, 2008; Accepted: July 21, 2008; DOI: 10.1002/marc.200800316

Keywords: chain disentanglement; drawing; in situ NMR measurement system; melt; polyethylene (PE)

[1] Z. Bashir, A. Keller, *Colloid Polym. Sci.* **1989**, *267*, 116.
[2] H. Uehara, M. Nakae, T. Kanamoto, A. E. Zachariades, R. S. Porter, *Macromolecules* **1999**, *32*, 2761.
[3] M. Nakae, H. Uehara, T. Kanamoto, T. Ohama, R. S. Porter, *J. Polym. Sci., Part B: Polym. Phys.* **1999**, *37*, 1921.
[4] M. Nakae, H. Uehara, T. Kanamoto, A. E. Zachariades, R. S. Porter, *Macromolecules* **2000**, *33*, 2632.
[5] M. Kakiage, M. Sekiya, T. Yamanobe, T. Komoto, S. Sasaki, S. Murakami, H. Uehara, *Polymer* **2007**, *48*, 7385.
[6] H. Uehara, M. Kakiage, T. Yamanobe, T. Komoto, S. Murakami, *Macromol. Rapid Commun.* **2006**, *27*, 966.
[7] M. Kakiage, T. Yamanobe, T. Komoto, S. Murakami, H. Uehara, *J. Polym. Sci., Part B: Polym. Phys.* **2006**, *44*, 2455.
[8] M. Kakiage, T. Yamanobe, T. Komoto, S. Murakami, H. Uehara, *Polymer* **2006**, *47*, 8053.
[9] M. Kakiage, M. Sekiya, T. Yamanobe, T. Komoto, S. Sasaki, S. Murakami, H. Uehara, *J. Phys. Chem.* **2008**, *112*, 5311.
[10] R. Folland, A. Charlesby, *J. Polym. Sci., Polym. Lett. Ed.* **1978**, *16*, 339.
[11] R. Folland, A. Charlesby, *Eur. Polym. J.* **1979**, *15*, 953.
[12] I. Kamel, A. Charlesby, *J. Polym. Sci., Polym. Phys. Ed.* **1981**, *19*, 803.
[13] M. Ito, T. Kanamoto, K. Tanaka, R. S. Porter, *Macromolecules* **1981**, *14*, 1779.
[14] J. P. Cohen-Addad, R. Dupeyre, *Polymer* **1983**, *24*, 400.
[15] H. Tanaka, T. Nishi, *J. Chem. Phys.* **1986**, *85*, 6197.
[16] M. Takenaka, T. Yamanobe, T. Komoto, I. Ando, H. Sato, K. Sato, *J. Polym. Sci., Part B: Polym. Phys.* **1987**, *25*, 2165.
[17] J. P. Cohen-Addad, G. Feio, A. Peguy, *Polym. Commun.* **1987**, *28*, 252.
[18] M. G. Brereton, I. M. Ward, N. Boden, P. Wright, *Macromolecules* **1991**, *24*, 2068.
[19] D. Dadayli, R. K. Harris, A. M. Kenwright, B. J. Say, M. M. Sunnetcioglu, *Polymer* **1994**, *35*, 4083.
[20] T. Bremner, A. Rudin, *J. Polym. Sci., Part B: Polym. Phys.* **1996**, *34*, 1893.
[21] L. S. Loo, R. E. Cohen, K. K. Gleason, *Macromolecules* **1999**, *32*, 4359.
[22] L. S. Loo, R. E. Cohen, K. K. Gleason, *Science* **2000**, *288*, 116.
[23] H. Uehara, T. Yamanobe, T. Komoto, *Macromolecules* **2000**, *33*, 4861.
[24] H. Uehara, H. Matsuda, T. Aoike, T. Yamanobe, T. Komoto, *Polymer* **2001**, *42*, 5893.
[25] R. C. Hedden, H. Tachibana, T. M. Duncan, C. Cohen, *Macromolecules* **2001**, *34*, 5540.
[26] H. Uehara, T. Aoike, T. Yamanobe, T. Komoto, *Macromolecules* **2002**, *35*, 2640.
[27] T. Kameda, T. Asakura, *Polymer* **2003**, *44*, 7539.
[28] J. Leisen, H. W. Beckham, M. A. Sharaf, *Macromolecules* **2004**, *37*, 8028.
[29] S. Rastogi, D. R. Lippits, G. W. M. Peters, R. Graf, Y. Yao, H. W. Spiess, *Nature Mat.* **2005**, *4*, 635.
[30] J. Rault, J. Marchal, P. Judeinstein, P. A. Albouy, *Macromolecules* **2006**, *39*, 8356.
[31] D. R. Lippits, S. Rastogi, G. W. H. Hohne, B. Mezari, P. C. M. M. Magusin, *Macromolecules* **2007**, *40*, 1004.
[32] H. Uehara, A. Uehara, M. Kakiage, H. Takahashi, S. Murakami, T. Yamanobe, T. Komoto, *Polymer* **2007**, *48*, 4547.
[33] S. Sasaki, K. Tashiro, M. Kobayashi, Y. Izumi, K. Kobayashi, *Polymer* **1999**, *40*, 7125.
[34] J. Zhang, Y. Duan, H. Sato, H. Tsuji, I. Noda, S. Yan, Y. Ozaki, *Macromolecules* **2005**, *38*, 8012.
[35] S. Watanabe, J. Dybal, K. Tashiro, Y. Ozaki, *Polymer* **2006**, *47*, 2010.
[36] L. Kurelec, S. Rastogi, R. J. Meier, P. J. Lemstra, *Macromolecules* **2000**, *33*, 5593.
[37] L. Brambilla, G. Zerbi, *Macromolecules* **2005**, *38*, 3327.
[38] S. Meiboom, D. Gill, *Rev. Sci. Instrum.* **1958**, *29*, 688.

DOI: 10.1002/marc.200800316